Accelerating and Premature Aging Characterizing Regional Cortical Volume Loss in Human Immunodeficiency Virus Infection: Contributions from Alcohol, Substance Use, and Hepatitis C Co-Infection

Supplemental Information

Supplemental Methods and Materials

Participants

Research clinicians administered the Structured Clinical Interview for DSM-IV (1) to all participants (2) after screening with a breathalyzer to ensure a current blood alcohol level of 0.0. Only participants meeting DSM-IV criteria for Alcohol Dependence were included in the HIV+Alc and Alc groups. Prospective controls did not meet DSM-IV criteria for any Axis I disorder. All participants were asked about quantity of lifetime alcohol consumed and date of last drink (3-5), and underwent a blood draw to determine HIV and HCV serological status, complete blood count, and comprehensive metabolic panel. HIV-infected subjects were included if their CD4 T-cell count was >40mm^3 and Karnofsky score was ≥70. Participants were excluded for chronic conditions that could affect brain structure, such as head trauma, sustained loss of consciousness, uncontrolled hypertension, and diabetes. Blood chemistry and other physiological data were available for most HIV-infected and Alc participants to enable deriving the Veterans Aging Cohort Risk (VACS) index of antiretroviral therapy responsiveness (6).

Past or current nicotine dependence had a higher incidence in the diagnostic groups than the control group. A large proportion in each diagnostic group also met historical DSM-IV

criteria for substance dependence (to cannabis, cocaine, amphetamines, or opiates): 29 (42.6%) HIV, 46 (76.7%) HIV+Alc, and 128 (57.7%) Alc. One control developed cannabis dependence at a later MRI but had no drug diagnosis at her initial visit. Only participants with serologically-confirmed HCV status were considered in analysis including 23/66 (34.8%) HIV, 31/59 (52.5%) HIV+Alc, 37/152 (24.3%) Alc, and 4/93 control participants (only the 89 HCV-negative controls were included in analyses related to HCV).

MRI Acquisition and Analysis

These methods presented next were described previously (7).

Image Acquisition

Structural MRI data were acquired between 11 April 2003 and 3 March 2017 on a 3 Tesla GE whole-body MR system (General Electric Healthcare, Waukesha, WI) using an 8-channel phased-array head coil. Throughout the years of data collection, an axial T1-weighted Inversion-Recovery Prepared SPoiled Gradient Recalled (SPGR) sequence was acquired. Parameters were consistent (e.g., inversion time (TI)=300 ms, matrix = 256x256, thickness=1.25 mm, skip=0 mm, 124 slices) or negligibly different (e.g., repetition time (TR)=6.55 or 5.92 ms, echo time (TE)=1.56 or 1.93 ms) across time. Routine phantom scans were used to evaluate spatial fidelity; drift was corrected by adjusting scanner calibration parameters when necessary to maintain spatial stability within manufacturer guidelines.

Image Processing

Preprocessing of T1-weighted MRI data involved noise removal (8) and brain mask segmentation using FSL BET(9), AFNI 3dSkullStrip (10), and Robust Brain Extraction (ROBEX) (11)

generating 3 brain masks. In parallel, noise-corrected, T1-weighted images were corrected for field inhomogeneity via N4ITK (12) and brain masks were segmented using the 3 methods listed above plus FreeSurfer mri_gcut (13). The resulting 7 segmented brain masks were reduced to one using majority voting (14).

Further processing focused on extracting longitudinal measurements from the skull-stripped, T1-weighted images. For each subject with multiple scans, an average intensity map for a single scan was computed by non-rigidly registering the skull-stripped T1-weighted images of all scans to the scan to be analyzed via symmetric, diffeomorphic, non-rigid registration using ANTS (15). Following this, average intensity maps across all scans were computed. To generate brain tissue segmentations (gray matter, white matter, cerebrospinal fluid), the average intensity maps of follow-up scans were rigidly aligned to the subject's baseline (i.e., first) scan via ANTS (15) before simultaneously segmenting all consequent scans via Atropos (16). Longitudinal metrics included regions defined by the SRI24 atlas (17) by non-rigidly registering the average intensity map of the first scan to the SRI24 atlas via ANTS (15).

To seek systematic effects of scanning date on MRI measures, we tested correlations between the supratentorial volume of controls at their first scan and the days since 2003 of these observations. This analysis yielded an r=.046, which was not significant (p=.344, df=419), thereby confirming our assumption about the stability of the scanner and its output over time.

HAND and Composite Scores

HIV-Associated Neurocognitive Disorder (HAND) is a categorical rating based on deviations from the means of composite scores representing 6 functional domains (cf., 18, 19).

Each of the composite scores was the mean of available test measures for each participant: Executive Function (EXF) comprised Trails B (20) or Color Trails 2 (21) time, WMS-R (22) or MicroCog (23) forward and backward digit span, and the Golden Stroop Color Word raw score (24); Learning/Memory (LM) comprised the Rey-Osterrieth Complex Figure Test immediate recall raw score (25) and WMS-R Logical Memory (immediate recall total raw score) (22) or MicroCog Memory (immediate recognition score) (23); Verbal/ Language (VL) comprised FAS letter fluency total score (26) and NART (27), Peabody (28), or WTAR (29) total score; Speed of Information Processing (SIP) comprised Trails A (20) or Color Trails 1(21) time, Digit Symbol (30) or Symbol Digit (31) raw score, and Golden Stroop Color raw score (25); Motor Skills (MS) comprised Grooved Pegboard mean of left and right hand scores (32), Fine Finger Movement mean of all conditions (33), and Ataxia mean score of standing on the left and right legs separately (34); Quality of Social Functioning (QSF) comprised Quality of Life SF-21 total raw score (35), Global Assessment of Functioning score (current) (36), and Activities of Daily Living (combined Performance and Instrumental scores) (37). Because of the longitudinal nature of this study, some tests supplanted others over time (e.g., Trail Making Test vs. Color Trails Test). All metrics (e.g., speed scores such as Trails A and B) were transformed so that higher scores were in the direction of better performance. Raw scores from tests included in each composite score were age-corrected based on 66 male and 85 female, healthy controls, aged 20 to 67 at their first examination and expressed as standardized Z-scores.

The HAND categorical score ranged from 0 to 3: 0 indicated normal performance; 1 indicated that scores on 2/5 composites were 1 standard deviation (SD) below the control mean, but QSF was 1 SD above the control mean; 2 indicated that 2/5 composite scores and the

QSF score were 1 SD below the control mean; and 3 indicated that 2/5 composites were 2 SD and QSF was 1 SD below the control mean.

Statistical Analysis

Primary statistical analyses were performed with R (38) and were based on linear or quadratic mixed effects models (*lmer*), which incorporated cross-sectional and longitudinal brain observations, to test primary variables of diagnosis, age, and sex (7). Follow-up t-tests examined differences between 2-group pairs.

The effect of intracranial volume on cortical volume. The magnitude of regional cortical gray matter volumes is highly correlated with supratentorial volume (svol). To examine each gray matter volume region of interest independent of svol, the regression of regional volume on svol was computed for controls with a general linear model (*lm* in R); this function was then applied to the data of all participants at each scan. Only controls were used in the fitting function to assure that the estimate of relation was not influenced by disease (cf.,39, 40). This procedure also minimized sex effects given that women, in general, have smaller heads and supratentorial volumes than men (mean svol for control women =1199.3cc vs control men 1360.5cc, t=11.397, $p<10^{-16}$ in the current sample) (7). Consequently, all brain volumes were svol-corrected to account for sex differences due solely to headsize differences.

The effect of diagnosis. The effect of diagnosis was examined for each brain volume with *lmer* as a function of diagnosis+age across all observations for all subjects and diagnoses. Dependence of volume on the interaction of diagnosis and age (diagnosis*age or

diagnosis*(age+age^2) was also examined. Similar analyses were performed for diagnosis+sex and diagnosis*sex.

Effects independent of age and sex. The effect of age on brain volumes was computed (*lmer*) for all control subjects for all observations. The results of this function were then used to compute age-independent observations for all participants regardless of diagnosis over all observations, producing a value, "age_predicted." Then we computed the mean, age-independent brain-volume values across all observations for each subject, to produce a single value, "age_predicted_mean." Sex effects were then removed with regression analysis (*lm*), using diagnosis as the independent variable, "age_predicted_mean" as the dependent variable, and sex as a covariate, producing "sex_age_predicted_mean." These age- and sex-independent brain volume data, expressed as a single value for each subject, were then used to examine the effects of substance dependence, HCV infection, and related variables.

Effect of HIV infection or drinking variables. Within each group, the age- and sex-independent brain values were used to examine the influence of drinking with t-tests for dichotomous drinking variables and correlations for continuous HIV or drinking variables.

Effect of drug-dependence history. Using the age- and sex-independent brain data for each of the three patient groups separately, drug-dependent (cocaine, cannabis, amphetamine, opiates) and non-drug dependent participants in each diagnostic group were tested against the 199 controls with a general linear model (*lm*) followed by analysis of variance (*anova*). These tests were repeated to determine the effects of drug-dependence vs. non-drug dependence within each primary diagnostic group.

Effect of HCV infection history. Using the age- and sex-independent brain data, diagnosis among those with known HCV infection status was tested with *lm* followed by *anova;* t-tests examined differences between group pairs.

Correlations between MRI volumes and HIV disease and neuropsychological test factors. Pearson correlations were calculated using age- and sex-independent brain volumes. P-values reported were adjusted using family-wise Bonferroni correction for directional results (one-tailed) with α=.05. Thus, for analyses based on 6 lobar regions, p≤.017; for analyses based on 30 regions, p≤.003.

Supplemental Information Table S1. Diagnosis and age-interaction effects on 30 regional volumes

	Total HIV Group (N=128)								HIV only Group (N=68)							
	Difference from controls				Group x age interaction				Difference from controls				Group x age interaction			
			R^2				R^2				R^2				R^2	
Region	t-test	FDR p-value	Fixed	Fixed+Random	t-test	FDR p-value	Fixed	Fixed+Random	t-test	FDR p-value	Fixed	Fixed+Random	t-test	FDR p-value	Fixed	Fixed+Random
Frontal_precentral	-5.727	**0.0000**	0.196	0.962	-3.265	**0.0109**	0.193	0.963	-4.753	**0.0000**	0.191	0.964	-3.779	**0.0012**	0.191	0.964
Frontal_superior	-4.287	**0.0001**	0.259	0.968	-4.464	**0.0002**	0.246	0.969	-3.799	**0.0009**	0.259	0.971	-4.818	**0.0000**	0.248	0.973
Frontal_orbital	-1.225	0.2462	0.047	0.983	-0.704	0.5777	0.045	0.983	0.503	0.6831	0.036	0.984	-0.360	0.8712	0.034	0.984
Frontal_middle	-4.494	**0.0000**	0.229	0.982	-3.118	**0.0136**	0.218	0.982	-3.562	**0.0011**	0.227	0.985	-3.591	**0.0020**	0.217	0.985
Frontal_inferior	-4.787	**0.0000**	0.122	0.988	1.088	0.4150	0.126	0.988	-4.917	**0.0000**	0.142	0.989	1.462	0.2695	0.147	0.989
Frontal_supp motor	-3.617	**0.0010**	0.142	0.986	-3.053	**0.0136**	0.131	0.986	-3.579	**0.0011**	0.150	0.985	-2.524	**0.0348**	0.140	0.986
Frontal_medial	-6.374	**0.0000**	0.249	0.982	-1.959	0.1186	0.241	0.982	-4.662	**0.0000**	0.218	0.983	-2.475	**0.0363**	0.210	0.984
Temporal_superior	-3.022	**0.0054**	0.057	0.988	0.478	0.7033	0.058	0.988	-3.634	**0.0011**	0.081	0.990	0.137	0.9218	0.081	0.990
Temporal_middle	-2.730	**0.0112**	0.191	0.989	1.106	0.4150	0.198	0.989	-1.588	0.1685	0.203	0.990	0.243	0.8978	0.204	0.990
Temporal_inferior	-2.029	0.0636	0.105	0.988	1.935	0.1186	0.115	0.989	-1.358	0.2275	0.113	0.990	1.859	0.1350	0.123	0.991
Parietal_postcentral	-4.736	**0.0000**	0.179	0.974	-1.976	0.1186	0.171	0.974	-3.666	**0.0011**	0.176	0.974	-2.568	**0.0341**	0.167	0.974
Parietal_superior	-3.792	**0.0006**	0.136	0.978	-0.088	0.9300	0.135	0.978	-2.170	0.0599	0.116	0.978	0.049	0.9606	0.116	0.978
Parietal_inferior	-3.079	**0.0048**	0.106	0.992	2.866	0.0167	0.121	0.992	-2.743	**0.0152**	0.113	0.992	3.092	0.0085	0.130	0.993
Parietal_supramarginal	-0.275	0.7835	0.080	0.983	2.794	0.0174	0.098	0.984	0.194	0.9065	0.082	0.984	3.440	0.0029	0.106	0.986
Parietal_precuneus	-3.390	**0.0021**	0.065	0.992	-0.432	0.7135	0.064	0.992	-1.790	0.1159	0.041	0.992	-0.623	0.7272	0.040	0.992
Parietal_paracentral	-1.925	0.0739	0.060	0.984	-1.886	0.1186	0.055	0.984	-1.828	0.1127	0.057	0.985	-1.182	0.3748	0.054	0.985
Occipital_calcarine	0.379	0.7292	0.000	0.984	1.891	0.1186	0.003	0.984	1.296	0.2439	0.006	0.985	1.312	0.3158	0.008	0.985
Occipital_cuneus	1.573	0.1446	0.008	0.980	3.665	0.0037	0.021	0.980	1.185	0.2832	0.006	0.980	4.313	0.0002	0.024	0.980
Occipital_lingual	-1.124	0.2798	0.005	0.980	1.481	0.2597	0.004	0.979	0.130	0.9276	0.003	0.981	1.599	0.2196	0.003	0.981
Occipital_lateral	3.232	0.0034	0.043	0.945	-0.271	0.8133	0.043	0.945	3.613	0.0011	0.061	0.946	-0.462	0.8402	0.059	0.947
Insula	-2.858	**0.0085**	0.031	0.978	-0.847	0.5177	0.030	0.978	-2.431	**0.0347**	0.026	0.978	-0.312	0.8712	0.026	0.978
Cingulate_anterior	-2.235	**0.0424**	0.027	0.996	-1.048	0.4209	0.026	0.996	-1.903	0.1006	0.025	0.995	-0.885	0.5642	0.024	0.995
Cingulate_midposterior	-2.009	0.0636	0.044	0.990	-2.439	**0.0442**	0.039	0.990	-1.518	0.1843	0.036	0.990	-1.964	0.1143	0.032	0.990
Hippocampus	-2.760	**0.0108**	0.046	0.981	0.944	0.4704	0.042	0.981	-1.435	0.2065	0.039	0.983	0.343	0.8712	0.037	0.983
Parahippocampus	3.122	0.0045	0.056	0.989	0.724	0.5777	0.055	0.989	3.460	0.0015	0.075	0.989	3.948	0.0008	0.073	0.989
Amygdala	1.711	0.1135	0.008	0.947	-1.173	0.4013	0.009	0.947	2.097	0.0675	0.016	0.952	-0.734	0.6613	0.016	0.952
Caudate	-1.222	0.2462	0.061	0.955	2.845	0.0167	0.055	0.955	0.006	0.9955	0.064	0.957	2.812	0.0185	0.061	0.957
Putamen	-1.235	0.2462	0.159	0.971	-1.421	0.2741	0.153	0.970	-0.763	0.5143	0.160	0.974	-1.345	0.3152	0.154	0.973
Pallidum	-2.104	0.0559	0.063	0.959	-2.896	**0.0167**	0.060	0.960	-2.205	0.0589	0.061	0.960	-2.293	0.0546	0.059	0.961
Thalamus	-4.480	**0.0000**	0.187	0.963	0.536	0.6830	0.189	0.963	-4.023	**0.0004**	0.204	0.963	0.176	0.9214	0.205	0.963

	HIV+AIc Group (N=60)								Alcoholic Group (N=222)							
	Difference from controls				Group x age interaction				Difference from controls				Group x age interaction			
			R^2				R^2				R^2				R^2	
Region	t-test	FDR p-value	Fixed	Fixed+Random	t-test	FDR p-value	Fixed	Fixed+Random	t-test	FDR p-value	Fixed	Fixed+Random	t-test	FDR p-value	Fixed	Fixed+Random
Frontal_precentral	-4.623	**0.0001**	0.146	0.969	-1.338	0.1809	0.142	0.969	-5.671	**0.0000**	0.131	0.974	-2.737	**0.0465**	0.144	0.973
Frontal_superior	-3.193	**0.0053**	0.191	0.977	-2.579	**0.0099**	0.180	0.977	-3.131	**0.0048**	0.149	0.983	-2.763	**0.0465**	0.162	0.983
Frontal_orbital	-2.843	**0.0134**	0.086	0.981	-0.918	0.3585	0.083	0.980	-1.814	0.0995	0.050	0.980	-0.716	0.6965	0.051	0.980
Frontal_middle	-3.741	**0.0009**	0.206	0.986	-1.324	0.1856	0.200	0.986	-2.763	**0.0118**	0.153	0.988	-0.663	0.6965	0.155	0.988
Frontal_inferior	-2.525	**0.0289**	0.088	0.987	0.092	0.9267	0.088	0.987	-2.318	**0.0361**	0.061	0.987	-0.622	0.6965	0.063	0.987
Frontal_supp motor	-2.282	0.0520	0.105	0.990	-2.987	**0.0028**	0.094	0.991	-4.115	0.0002	0.096	0.990	-1.700	0.2057	0.099	0.990
Frontal_medial	-5.465	**0.0000**	0.218	0.983	-0.506	0.6128	0.215	0.983	-4.481	**0.0001**	0.145	0.986	-1.857	0.1727	0.151	0.986
Temporal_superior	-0.961	0.3739	0.027	0.988	0.681	0.4957	0.029	0.988	-2.865	**0.0096**	0.041	0.989	-0.186	0.9443	0.041	0.989
Temporal_middle	-2.743	**0.0166**	0.202	0.990	1.975	0.0482	0.213	0.990	-2.914	**0.0089**	0.157	0.988	3.075	0.0316	0.157	0.988
Temporal_inferior	-1.715	0.1364	0.111	0.990	1.637	0.1017	0.119	0.990	-1.872	0.0918	0.089	0.988	1.746	0.2022	0.088	0.988
Parietal_postcentral	-3.925	**0.0007**	0.135	0.981	-0.384	0.7009	0.134	0.981	-4.165	**0.0002**	0.096	0.984	-0.654	0.6965	0.096	0.984
Parietal_superior	-3.974	**0.0007**	0.154	0.980	-0.238	0.8121	0.153	0.980	-3.737	**0.0008**	0.108	0.983	0.120	0.9443	0.107	0.983
Parietal_inferior	-1.997	0.0810	0.106	0.992	1.455	0.1458	0.113	0.992	-4.246	**0.0002**	0.110	0.993	2.248	0.1054	0.110	0.993
Parietal_supramarginal	-0.537	0.6116	0.118	0.986	1.072	0.2837	0.124	0.986	-0.993	0.3700	0.074	0.981	3.082	0.0316	0.078	0.981
Parietal_precuneus	-3.763	**0.0009**	0.081	0.992	-0.015	0.9877	0.081	0.992	-3.148	**0.0048**	0.038	0.993	0.793	0.6756	0.038	0.993
Parietal_paracentral	-1.265	0.2377	0.050	0.984	-1.952	0.0509	0.045	0.983	-3.194	0.0047	0.053	0.988	-0.508	0.7645	0.053	0.988
Occipital_calcarine	-0.807	0.4496	0.002	0.989	1.678	0.0934	0.003	0.989	1.097	0.3274	0.003	0.992	0.843	0.6647	0.004	0.992
Occipital_cuneus	1.588	0.1604	0.022	0.984	1.231	0.2183	0.026	0.984	1.761	0.1066	0.016	0.989	1.864	0.1727	0.017	0.989
Occipital_lingual	-2.029	0.0796	0.015	0.988	0.460	0.6452	0.015	0.988	-0.455	0.7215	0.006	0.989	1.541	0.2642	0.008	0.990
Occipital_lateral	1.459	0.1972	0.029	0.968	-0.221	0.8248	0.028	0.968	1.499	0.1747	0.012	0.977	2.522	0.0701	0.017	0.977
Insula	-2.058	0.0793	0.020	0.979	-1.236	0.2164	0.020	0.980	-4.920	**0.0000**	0.058	0.983	-1.924	0.1727	0.061	0.983
Cingulate_anterior	-1.599	0.1604	0.019	0.997	-0.873	0.3825	0.018	0.997	-2.736	**0.0118**	0.020	0.996	1.862	0.1727	0.021	0.996
Cingulate_midposterior	-1.741	0.1361	0.036	0.990	-2.091	**0.0365**	0.033	0.990	-2.282	0.0361	0.028	0.990	-1.148	0.5022	0.029	0.990
Hippocampus	-2.987	**0.0094**	0.060	0.984	1.268	0.2046	0.056	0.984	-2.732	**0.0118**	0.046	0.985	-1.015	0.5472	0.045	0.985
Parahippocampus	1.310	0.2284	0.025	0.991	-0.173	0.8625	0.026	0.991	1.184	0.2956	0.019	0.992	0.120	0.9443	0.019	0.992
Amygdala	0.435	0.6638	0.001	0.951	-1.197	0.2313	0.002	0.950	-0.355	0.7674	0.000	0.953	-0.021	0.9833	0.000	0.953
Caudate	-2.060	0.0793	0.063	0.965	1.942	0.0521	0.057	0.965	0.330	0.7674	0.043	0.975	0.170	0.9443	0.043	0.976
Putamen	-1.376	0.2154	0.169	0.968	-0.851	0.3948	0.165	0.968	0.181	0.8563	0.135	0.971	-0.110	0.9443	0.135	0.971
Pallidum	-1.365	0.2154	0.046	0.954	-2.346	**0.0190**	0.045	0.955	-2.276	0.0361	0.034	0.963	-1.082	0.5238	0.036	0.963
Thalamus	-3.396	**0.0029**	0.195	0.955	0.631	0.5282	0.198	0.955	-3.393	**0.0026**	0.197	0.956	-2.269	0.1054	0.209	0.955

bold=significant, FDR-corrected p-value with t-test in predicted direction

R^2 provides estimates of effect sizes, where R^2 <.01 is trivial, >.01 - .09 is small to medium, >.09 - .25 is medium to large, >.25 is large to very large.

xxx	Different from controls, no interaction
xxx	Age-by-diagnosis interaction
xxx	Blue font=alcoholics only different from controls

Supplemental Information Table S2. Effects of HIV-infection without alcohol, drug, or HCV comorbidities on 30 regional brain volumes

	199 Controls vs. 24 HIV (no alcohol, drugs, HCV)[a]					
	Group differences			Age interactions		
Lobar region	**t-value**	**p-value**	**FDR p-value**	**group x age**	**p-value**	**FDR p-value**
Frontal	-2.619	0.0088	*0.0529*	-3.801	0.0001	**0.0004**
Temporal	0.142	0.8869	0.8869	-0.419	0.6750	0.6750
Parietal	-0.791	0.4291	0.5149	-1.421	0.1555	0.2332
Occipital	1.016	0.3095	0.5149	0.643	0.5199	0.6239
Insula	-1.303	0.1926	0.5149	-1.467	0.1425	0.2332
Cingulate	-0.838	0.4022	0.5149	-2.223	0.0262	0.0786
Subregion	**t-value**	**p-value**	**FDR p-value**	**group x age**	**p-value**	**FDR p-value**
Frontal_precentral	0.737	0.4612	0.6427	-4.955	0.0000	**0.0000**
Frontal_superior	-3.155	0.0016	**0.0377**	-5.173	0.0000	**0.0000**
Frontal_orbital	0.377	0.7061	0.8826	-0.831	0.4063	0.5540
Frontal_middle	-1.415	0.1570	0.4282	-4.243	0.0000	**0.0002**
Frontal_inferior	-2.060	0.0394	0.2366	0.137	0.8914	0.9221
Frontal_supplementary motor	-0.976	0.3290	0.5806	-2.075	0.0380	0.1265
Frontal_medial	-2.195	0.0282	0.2111	-2.661	0.0078	**0.0389**
Temporal_superior	-1.978	0.0479	0.2397	-0.003	0.9978	0.9978
Temporal_middle	1.012	0.3115	0.5806	-0.542	0.5878	0.7054
Temporal_inferior	0.748	0.4542	0.6427	0.617	0.5372	0.6715
Parietal_postcentral	-1.545	0.1223	0.3691	-3.960	0.0001	**0.0005**
Parietal_superior	-0.049	0.9606	0.9937	-1.174	0.2405	0.4221
Parietal_inferior	-1.648	0.0994	0.3691	1.004	0.3154	0.4848
Parietal_supramarginal	-0.720	0.4713	0.6427	2.188	0.0287	0.1076
Parietal_precuneus	1.096	0.2730	0.5806	-1.514	0.1300	0.2785
Parietal_paracentral	-0.137	0.8912	0.9902	-1.861	0.0627	0.1710
Occipital_calcarine	0.083	0.9340	0.9937	0.856	0.3919	0.5540
Occipital_cuneus	0.246	0.8054	0.9293	3.605	0.0003	0.0019
Occipital_lingual	0.323	0.7470	0.8964	1.651	0.0988	0.2280
Occipital_lateral	1.564	0.1178	0.3691	-1.143	0.2533	0.4221
Insula	-1.303	0.1926	0.4815	-1.467	0.1425	0.2850
Cingulate_anterior	-1.124	0.2609	0.5806	-1.741	0.0817	0.2043
Cingulate_midposterior	-0.007	0.9944	0.9944	-1.998	0.0457	0.1372
Hippocampus	-0.404	0.6860	0.8826	0.478	0.6327	0.7300
Parahippocampus	3.022	0.0025	0.0377	0.988	0.3232	0.4848
Amygdala	0.857	0.3912	0.6427	-1.299	0.1941	0.3639
Caudate	0.799	0.4241	0.6427	0.151	0.8803	0.9221
Putamen	-0.985	0.3245	0.5806	-2.222	0.0263	0.1076
Pallidum	0.026	0.1230	0.3691	-0.709	0.4786	0.6243
Thalamus	-2.476	0.0133	0.1328	-0.359	0.7198	0.7998

[a]controls=199 at initial MRI and 417 total MRIs; HIV without comorbidities=24 at initial MRI and 65 total MRIs
bold=FDR p-values≤0.05 in predicted direction (control>HIV mean; age interaction steeper in HIV than controls

xxx Age-by-diagnosis interaction

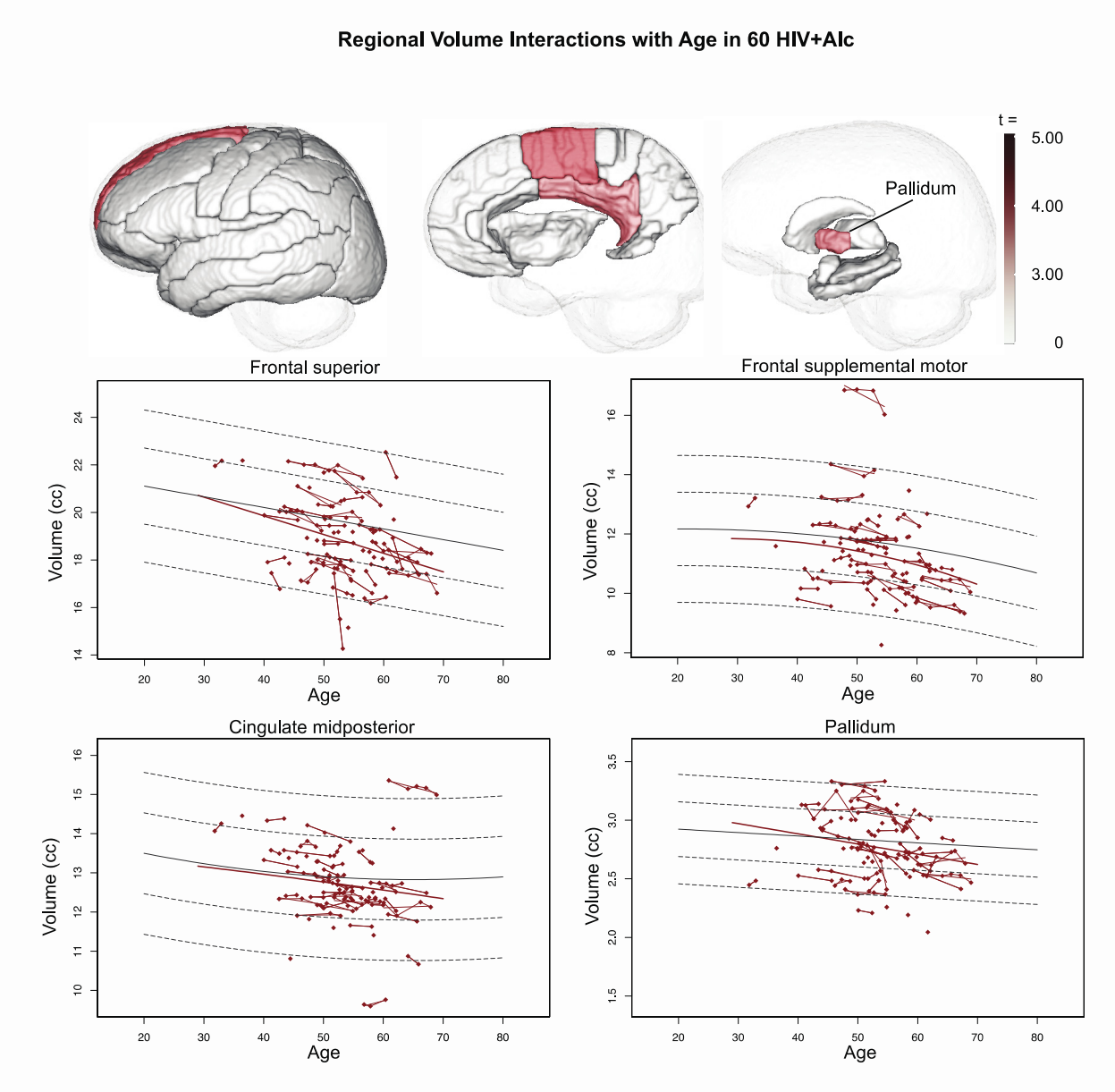

Supplemental Figure S1. Color-coded brain regions and scatterplots of significant age-diagnosis interactions in the HIV+Alc group indicating age-related declines in excess of those detected in the controls (gray regression lines).

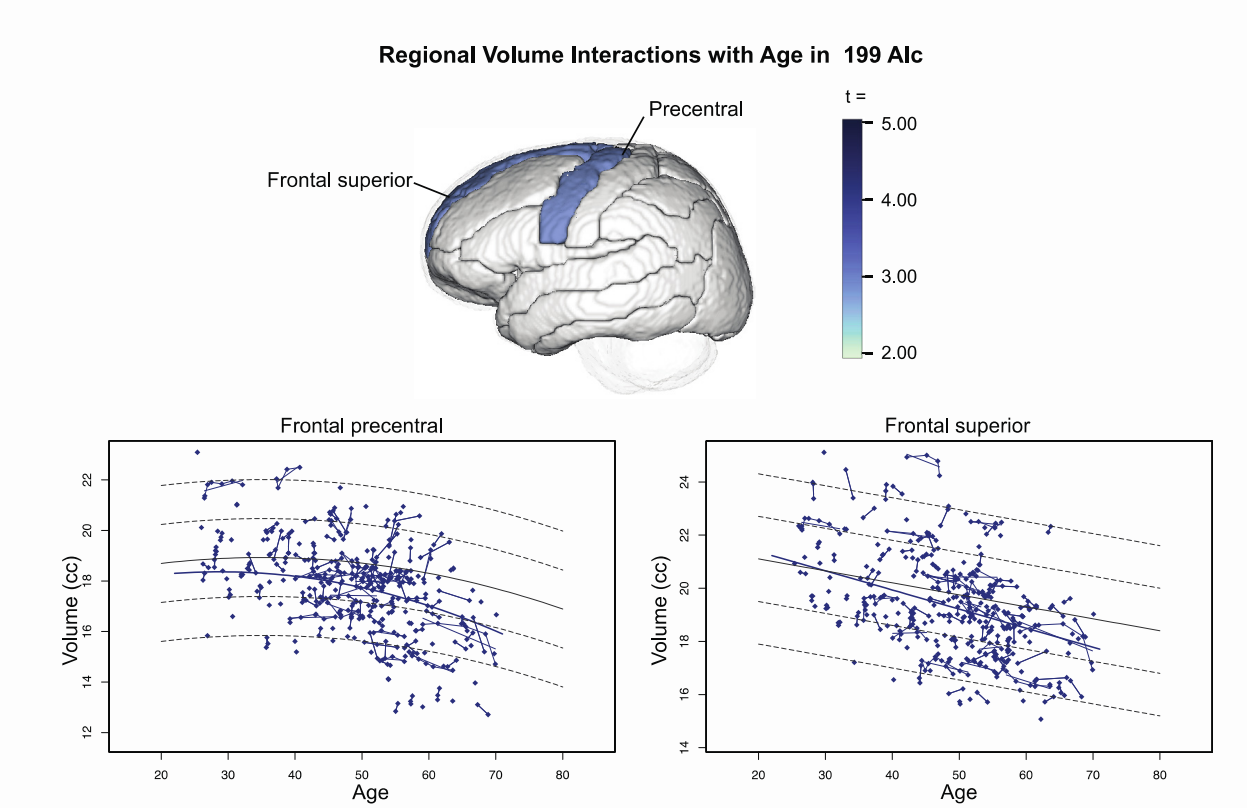

Supplemental Figure S2. Color-coded brain regions and scatterplots of significant age-diagnosis interactions in the Alc group only indicating age-related declines in excess of those detected in the controls (gray regression lines).

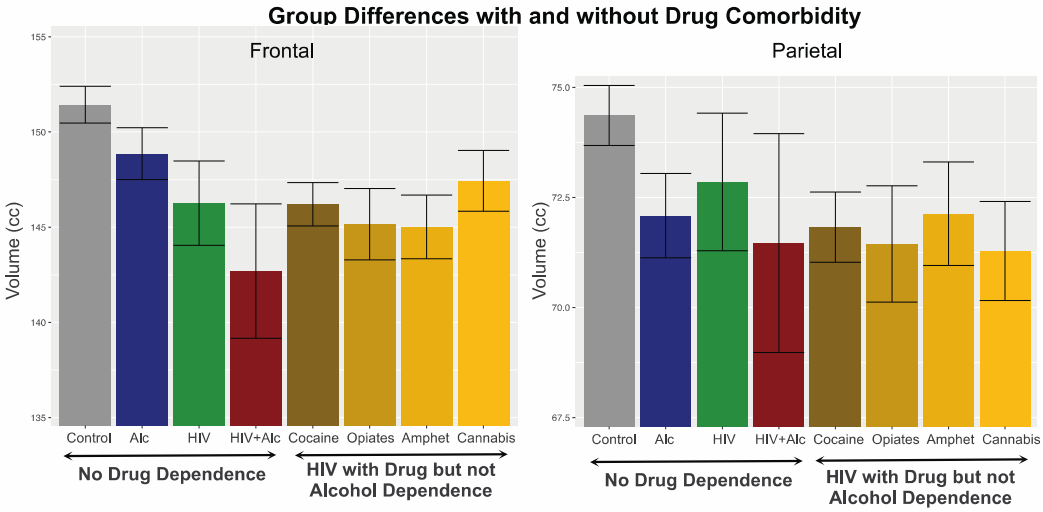
Group Differences with and without Drug Comorbidity
Frontal
Parietal
Volume (cc)
155
150
145
140
135
75.0
72.5
70.0
67.5
Control
Alc
HIV
HIV+Alc
Cocaine
Opiates
Amphet
Cannabis
No Drug Dependence
HIV with Drug but not Alcohol Dependence

Group Differences with and without HCV Comorbidity

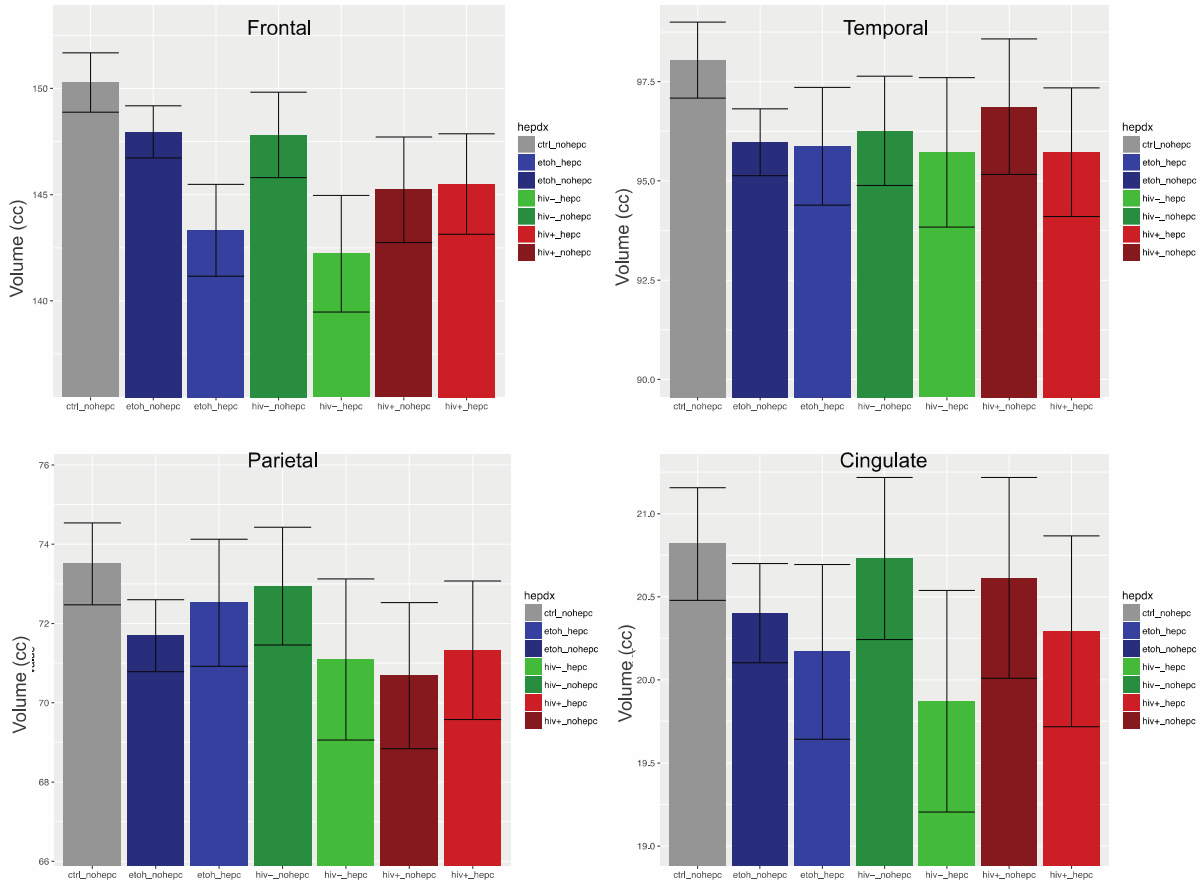

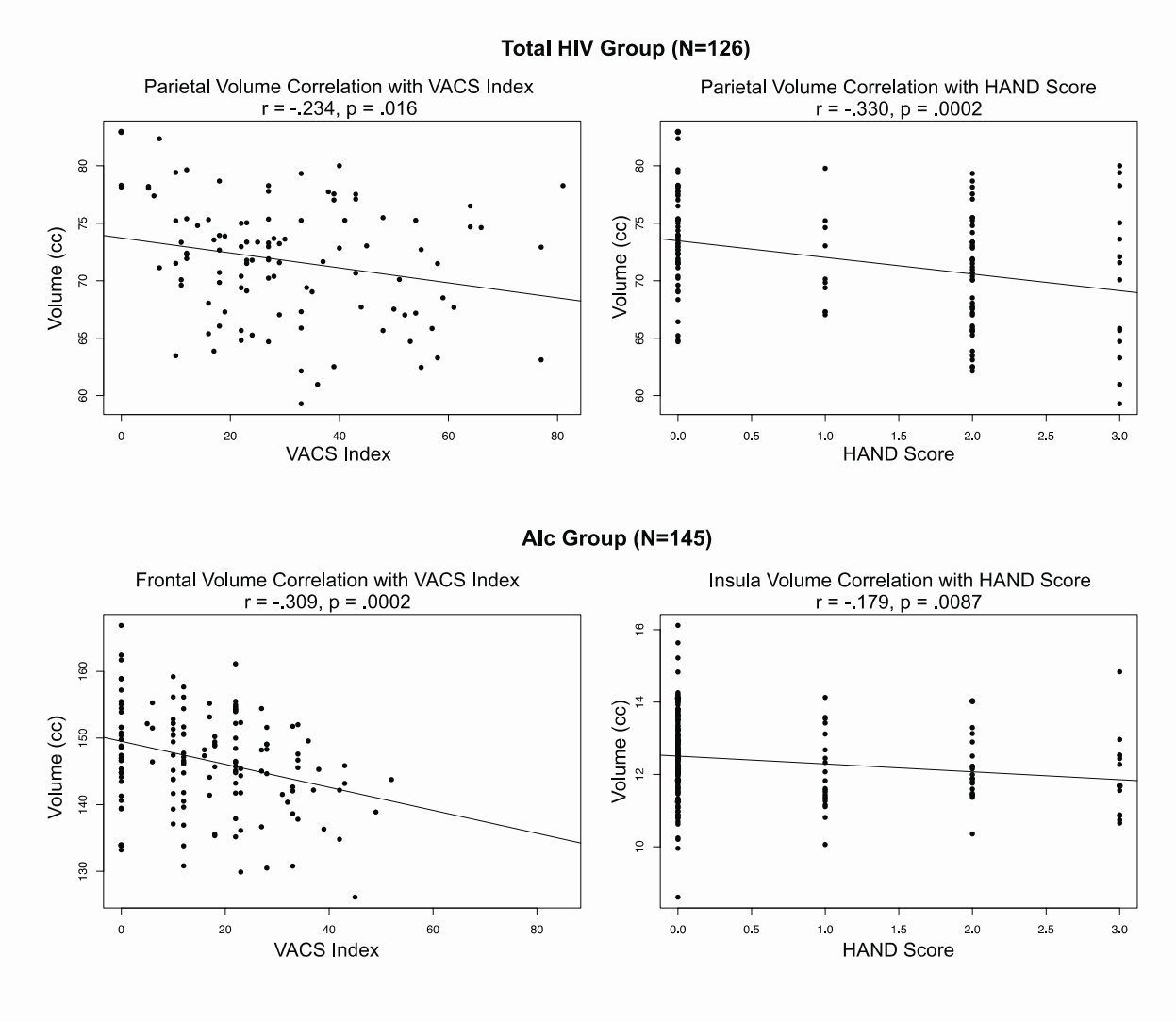

Supplemental Figure S5. Scatterplots of significant correlations between VACS or HAND scores and regional volumes in the total HIV group (top) and AIc group (bottom).

Supplemental References

1. First M (2000): *Diagnostic and Statistical Manual of Mental Disorders, Fourth Edition, Text Revision (DSM-IV-TR)*. Washington, DC: American Psychiatric Association.
2. Pfefferbaum A, Rogosa DA, Rosenbloom MJ, Chu W, Sassoon SA, Kemper CA, et al. (2014): Accelerated aging of selective brain structures in human immunodeficiency virus infection: a controlled, longitudinal magnetic resonance imaging study. *Neurobiology of aging*.
3. Pfefferbaum A, Lim KO, Rosenbloom MJ (1992): Structural imaging of the brain in chronic alcoholism. In: Zakhari S, Witt E, editors. *Imaging in Alcohol Research: NIAAA Research Monograph No 21*. Rockville, MD: U.S. Dept Health and Human Services, pp 99-120.
4. Skinner HA (1982): *Development and Validation of a Lifetime Alcohol Consumption Assessment Procedure*. Toronto, Canada: Addiction Research Foundation.
5. Skinner HA, Sheu WJ (1982): Reliability of alcohol use indices: The lifetime drinking history and the MAST. *Journal of Studies on Alcohol*. 43:1157-1170.
6. Brown ST, Tate JP, Kyriakides TC, Kirkwood KA, Holodniy M, Goulet JL, et al. (2014): The VACS index accurately predicts mortality and treament response amon multi-drug resistant HIV infected patients participating in the Options in Management with Antiretrovirals (OPTIMA) study. *PloS one*. 9:e92606.
7. Sullivan EV, Zahr NM, Sassoon SA, Thompson WK, Kwon D, Pohl KM, et al. (2018): Enduring Cortical Compromise in Alcoholism: Accelerated by Aging and Compounded by Drug Dependence and Hepatitis C Comorbidity. *Journal of the American Medical Association*. in revision.
8. Coupe P, Yger P, Prima S, Hellier P, Kervrann C, Barillot C (2008): An optimized blockwise nonlocal means denoising filter for 3-D magnetic resonance images. *IEEE transactions on medical imaging*. 27:425-441.
9. Smith S (2002): Fast robust automated brain extraction. *Human Brain Mapping*. 17:143-155.
10. Cox RW (1996): AFNI: software for analysis and visualization of functional magnetic resonance neuroimages. *Comput Biomed Res*. 29:162-173.
11. Iglesias JE, Liu CY, Thompson PM, Tu Z (2011): Robust brain extraction across datasets and comparison with publicly available methods. *IEEE transactions on medical imaging*. 30:1617-1634.
12. Tustison NJ, Avants BB, Siqueira M, Gee JC (2011): Topological well-composedness and glamorous glue: a digital gluing algorithm for topologically constrained front propagation. *IEEE transactions on image processing : a publication of the IEEE Signal Processing Society*. 20:1756-1761.
13. Sadananthan SA, Zheng W, Chee MW, Zagorodnov V (2010): Skull stripping using graph cuts. *Neuroimage*. 49:225-239.

14. Rohlfing T, Brandt R, Menzel R, Maurer CR, Jr. (2004): Evaluation of atlas selection strategies for atlas-based image segmentation with application to confocal microscopy images of bee brains. *Neuroimage*. 21:1428-1442.

15. Avants BB, Epstein CL, Grossman M, Gee JC (2008): Symmetric diffeomorphic image registration with cross-correlation: evaluating automated labeling of elderly and neurodegenerative brain. *Medical image analysis*. 12:26-41.

16. Avants BB, Tustison NJ, Song G, Cook PA, Klein A, Gee JC (2011): A reproducible evaluation of ANTs similarity metric performance in brain image registration. *Neuroimage*. 54:2033-2044.

17. Rohlfing T, Zahr NM, Sullivan EV, Pfefferbaum A (2010): The SRI24 multi-channel atlas of normal adult human brain structure. *Human Brain Mapping*. 31:798-819.

18. Antinori A, Arendt G, Becker JT, Brew BJ, Byrd DA, Cherner M, et al. (2007): Updated research nosology for HIV-associated neurocognitive disorders. *Neurology*. 69:1789-1799.

19. Sacktor N, Skolasky RL, Seaberg E, Munro C, Becker JT, Martin E, et al. (2016): Prevalence of HIV-associated neurocognitive disorders in the Multicenter AIDS Cohort Study. *Neurology*. 86:334-340.

20. Tombaugh TN (2004): Trail Making Test A and B: normative data stratified by age and education. *Archives of clinical neuropsychology : the official journal of the National Academy of Neuropsychologists*. 19:203-214.

21. D'Elia L, Satz P (1989): *Color Trails 1 and 2*. Odessa, FL: Psychological Assessment Resources.

22. Bowden SC, Bell RC (1992): Relative usefulness of the WMS and WMS-R: a comment on D'Elia et al. (1989). *Journal of clinical and experimental neuropsychology*. 14:340-346.

23. Elwood RW (2001): MicroCog: assessment of cognitive functioning. *Neuropsychology review*. 11:89-100.

24. Golden C (1978): *Stroop Color and Word Test: A Manual for Clinical and Experimental Uses*. Chicago: Stoelling Co.

25. Bennett-Levy J (1984): Determinants of performance on the Rey-Osterrieth complex figure test: An analysis, and a new technique for single-case assessment. *British Journal of Clinical Psychology*. 23:109-119.

26. Borkowski JG, Benton AL, Spreen O (1967): Word fluency and brain damage. *Neuropsychologia*. 5:135-140.

27. Nelson HE (1982): *The National Adult Reading Test (NART)*. Windsor, Canada: Nelson Publishing Company.

28. Dunn LM, Dunn ES (1997): *Peabody Picture Vocabulary Test - Third Edition*. Circle Pines, MN: American Guidance Service.

29. Wechsler D (2001): Wechsler Test of Adult Reading: WTAR. San Antonio, TX: Pearson Education, Inc.

30. Hart R, Kwentus J, Wade J, Hamer R (1987): Digit symbol performance in mild dementia and depression. *Journal of Consulting and Clinical Psychology*. 55:236-238.

31. Smith A (1973): *The Symbol Digit Modalities Test Manual*. Los Angeles: Western Psychological Services.

32. Trites RL (1977): The Grooved Pegboard Test. *Neuropsychological Test Manual*. Ontario, Canada: Royal Ottawa Hospital.

33. Fama R, Eisen JC, Rosenbloom MJ, Sassoon SA, Kemper CA, Deresinski S, et al. (2007): Upper and lower limb motor impairments in alcoholism, HIV infection, and their comorbidity. *Alcoholism, clinical and experimental research*. 31:1038-1044.

34. Fregly AR (1968): An ataxia battery not requiring rails. *Aerospace Medicine*. 39:277-282.

35. Bozzette SA, Hays RD, Berry SH, Kanouse DE, Wu AW (1995): Derivation and properties of a brief health status assessment instrument for use in HIV disease. *Journal of acquired immune deficiency syndromes and human retrovirology : official publication of the International Retrovirology Association*. 8:253-265.

36. Moos RH, McCoy L, Moos BS (2000): Global assessment of functioning (GAF) ratings: determinants and role as predictors of one-year treatment outcomes. *Journal of Clinical Psychology*. 56:449-461.

37. Katz S (1983): Assessing self-maintenance activities of daily living, mobility and instrumental activities of daily living. *Journal of the American Geriatric Society*. 31:721-727.

38. R Core Team (2013): R: A language and environment for statistical computing. . Vienna, Austria: R Foundation for Statistical Computing.

39. Pfefferbaum A, Lim KO, Zipursky RB, Mathalon DH, Lane B, Ha CN, et al. (1992): Brain gray and white matter volume loss accelerates with aging in chronic alcoholics: A quantitative MRI study. *Alcoholism: Clinical and Experimental Research*. 16:1078-1089.

40. Mathalon DH, Sullivan EV, Rawles JM, Pfefferbaum A (1993): Correction for head size in brain-imaging measurements. *Psychiatry Research: Neuroimaging*. 50:121-139.